

Pinpointing Chiral Structures with Front-Back Polarized Neutron Reflectometry

K. V. O'Donovan,^{1,*} J. A. Borchers,¹ C. F. Majkrzak,¹ O. Hellwig,² and E. E. Fullerton²

¹NIST Center for Neutron Research, National Institute of Standards and Technology, Gaithersburg, Maryland 20899

²IBM Almaden Research Facility, 650 Harry Road, San Jose, California 95120

(Received 16 February 2001; published 25 January 2002)

A new development in spin-polarized neutron reflectometry enables us to more fully characterize the nucleation and growth of buried domain walls in layered magnetic materials. We applied this technique to a thin-film exchange-spring magnet. After first measuring the reflectivity with the neutrons striking the front, we measure with the neutrons striking the back. Simultaneous fits are sensitive to the presence of spiral spin structures. The technique reveals previously unresolved features of field-dependent domain walls in exchange-spring systems and has sufficient generality to apply to a variety of magnetic systems.

DOI: 10.1103/PhysRevLett.88.067201

PACS numbers: 75.25.+z, 61.12.Ha, 75.60.Ch, 75.70.-i

Of late there has been a tremendous increase in the investigation of the magnetic properties of exchange-coupled systems. These systems range from exchange-biased systems of ferromagnets and antiferromagnets [1] to exchange-spring systems of soft and hard ferromagnets [2–5]. Features of spin-dependent transport in many systems are related to the growth and movement of domain walls and the reorientation of the moment direction near the relevant interfaces [1,4,6]. The development of sensors and magnetic recording devices can be accelerated once we understand the physics of confined domain walls.

Techniques to image the moment, such as scanning electron microscopy with polarization analysis (SEMPA) [7], magneto-optical Kerr effect (MOKE) [8], and magneto-optical indicator film (MOIF) imaging [9] are surface sensitive, and/or average the moment over the 10 to 50 nm thickness of the magnetic modulations. Polarized neutron reflectometry (PNR) senses the magnetic variations over these dimensions throughout the full depth of the sample, but it cannot always discriminate among several physically reasonable structures.

We have developed an adaptation of the PNR technique which provides increased sensitivity to magnetic spirals, yet adds no complexity to the experimental setup. We measure the reflectivity first with the scattering vector \mathbf{Q} pointing away from the front of the sample and then with \mathbf{Q} pointing away from the back of the sample. We then fit both data sets simultaneously. We have applied this technique to a bilayer exchange-spring magnet $\text{Ni}_{80}\text{Fe}_{20}|\text{Fe}_{55}\text{Pt}_{45}$ in order to fully image the field evolution of a domain wall in buried magnetic layers.

The recent developments in the area of magnetic microelectromechanical systems (MEMS) brings to the fore the need for miniaturized permanent magnets. Today's layered exchange-spring systems build upon the concept introduced by Kneller and Hawig [2]. Thin layers of a highly anisotropic hard ferromagnet alternate with those of a highly remanent soft ferromagnet. In modest reversed fields a domain wall some 10 nm thick creates a twist in the soft ferromagnet, while the hard ferromagnet lies pinned.

Once the field is removed, the soft ferromagnet recovers its original magnetization. At high fields the domain wall invades the hard ferromagnet and reversibility is lost. We observed the twist to the exclusion of other reasonable spin configurations, e.g., a uniform rotation throughout the sample. Furthermore, we have determined the Bloch wall invades the hard ferromagnet, as recent MOKE experiments suggest [8], even at fields in which the magnetization is ostensibly reversible.

The sample studied is a polycrystalline bilayer film prepared by magnetron sputtering on a glass substrate. A 1.5 nm seed layer is followed by 20.0 nm $\text{Fe}_{55}\text{Pt}_{45}$, 50.0 nm $\text{Ni}_{80}\text{Fe}_{20}$ (permalloy), and capped with Pt. Further details, and bulk magnetization measurements suggesting exchange-spring coupling between the soft NiFe and the hard FePt, can be found in [8] and references therein. The structural parameters were refined by measuring and fitting x-ray reflectivity.

The magnetic structure was determined by polarized neutron reflectometry, which probes the interaction between the neutron's magnetic moment and the magnetization of the sample. We used neutrons of wavelength 0.475 nm with the NG-1 reflectometer at the NIST Center for Neutron Research at the National Institute of Standards and Technology. The geometry of the experiment is shown in the right-hand inset in Fig. 1. The z - y scattering plane is horizontal with the outward normal to the front surface lying along the z axis. Control and detection of the incident and scattered neutron spin state are described elsewhere [10]. The neutrons are polarized along the vertical x axis, and the data are corrected for the efficiencies of the polarizing elements and the magnet [10], as well as for the footprint of the beam. Before correction, the efficiency ranges from 90% to 100%.

The reflectivities R^{++} and R^{--} , in which the polarized neutron does not change its orientation, sense the chemical structure of the bilayer (via scattering from the nuclei) and the x component of the magnetization \mathbf{M} ; they are designated as non-spin-flip (NSF) scattering. The reflectivities R^{+-} and R^{-+} are nonzero only when components of \mathbf{M}

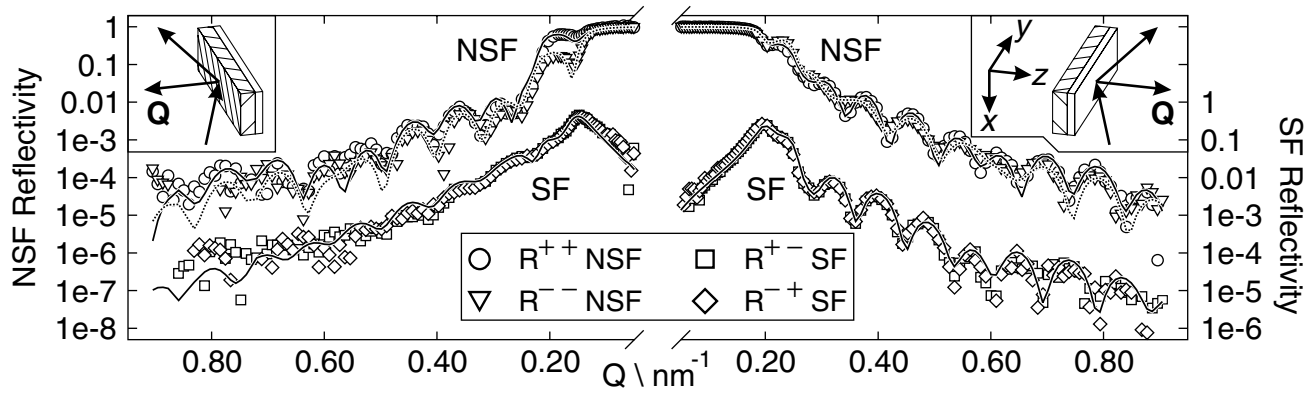


FIG. 1. Reflectivity at 16 mT. Data from the front (back) surface are shown on the right (left) with Q increasing towards the right (left). The non-spin-flip (NSF) data are plotted against the left axis. Differences in the two front NSF reflectivities are masked by the size and density of the symbols in the plot. The spin-flip (SF) data are plotted against the right axis, which is shifted by 2 orders of magnitude. For the back surface, when $Q > 0.62 \text{ nm}^{-1}$, the uncertainty in R is equal to or greater than R . Fits are shown as a dashed line for R^{-} and solid lines for R^{++} and R^{SF} . The insets show the scattering geometry for the two experimental configurations, with the incident and exit wave vectors unlabeled, and the momentum transfer Q labeled.

lie perpendicular to x , and are not particularly sensitive to the chemical structure; they are designated as spin-flip (SF) scattering.

The magnetic state of the sample was prepared by applying a field of 890 mT along the $+x$ axis, followed by 890 mT along $-x$. This sequence uniformly magnetizes the sample along $-x$. We measured the room-temperature PNR with a smaller field H applied along $+x$. The appearance of a Bloch wall parallel to the surface should twist the moment in the soft ferromagnet along $z \parallel Q$. Our data were measured at the following values of H : 5, 10, 16, 20, 26, 50, 100, 260, 350, and 630 mT (which is the uniformly magnetized state). Full details of the field evolution and remanence are forthcoming [11].

The first experiments were conducted with $H = 16 \text{ mT}$ and the neutrons glancing off the front surface. All four reflectivities were measured and are plotted on the right-hand portion of Fig. 1. Under the geometry we described above, we expect the two SF reflectivities to be identical, as we observe. The reflectivity from the back surface was measured by scanning in the negative direction; hence no repositioning of the sample is necessary to measure these data. Incoherent scattering of neutrons in the glass substrate reduces the intensity of the signal and introduces a higher background in the data on the left.

To minimize the number of free parameters in the fit, we use the following model which describes the principal features in the reflectivity. The top of the NiFe and the bottom of the FePt are assumed to have a uniform direction of moment throughout a variable thickness t_s and t_h , respectively. The moments make angles ϕ_s and ϕ_h with respect to the $+x$ axis and are allowed to vary freely. The spiral is characterized by a constant angular gradient ω_s in NiFe and ω_h in FePt with $|\omega_i| = |\phi_{\text{int}} - \phi_i|/(d_i - t_i)$, where ϕ_{int} is the fitted interfacial angle and d_i is the chemical thickness of component i . In the geometry used in this

experiment, we cannot determine the sign of ω , and thus the chirality of the spiral is unknown. We will address this matter in future experiments. The NiFe and FePt are subdivided into six or fewer sublayers in order to permit a variation of the size of the magnetization.

The agreement between the fit and the data (as plotted in Fig. 1) is excellent up to $Q = 0.70 \text{ nm}^{-1}$. The existence of SF reflectivity comparable to the NSF reflectivity indicates a significant fraction of the magnetization lies perpendicular to the applied field. Fitting just the front- or back-surface reflectivity leaves some uncertainty as to whether the spins are uniformly canted to the field with $\phi_s = \phi_h$. However, compare the NSF reflectivities at $Q = 0.20 \text{ nm}^{-1}$. The difference between the back-surface NSF reflectivities is much greater than that of the front-surface reflectivities. Increasing the field to 26 mT from 16 mT interchanges this front-back asymmetry. Having simulated a variety of magnetic structures for our sample, we conclude this asymmetric splitting characterizes non-collinear structures: $\phi_s \neq \phi_h$. Collinear magnetization of NiFe and FePt produces a symmetric splitting of the two NSF reflectivities. Fits to the features above the critical angle select a spiral ($\omega_i \neq 0$) rather than structures with, e.g., $t_i = d_i$, $\phi_h = 180^\circ$, and $\phi_s = 90^\circ, 180^\circ$, or 270° , even when multiple domains with these structures scatter incoherently. The damped oscillations in the back-surface SF reflectivity (relative to the front) also support nonzero ω [11].

Measuring the back reflectivity is akin to holding the front surface of the bilayer up to a mirror to see whether the mirror image is the same as the original structure. In a collinear structure all the spins are aligned along a common direction, and the mirror image is very much like the original structure. But the mirror image of a magnetic twist to the right is a magnetic twist to the left. Therefore, if the front and back reflectivities are significantly different,

we can deduce the presence of a spiral. But to reiterate, we cannot determine the chirality of the spiral, only its presence. Rühm's formulation of reflectivity [12] shows that $R^{\text{NSF}} = |R_0 + R_\xi P_\xi + R_\zeta P_\zeta + R_\eta P_\eta|^2/4$ with neutron polarization \mathbf{P} . The Cartesian coordinate system $\{\xi, \zeta, \eta\}$ has $\eta = z$ and ξ lies along the net magnetization in the sample. It can be shown that measuring the back reflectivity of trivial noncollinear bilayers is equivalent to rotating \mathbf{P} 180° about ξ [11]. P_ζ and P_η change sign while P_ξ is invariant under this rotation. Because ξ often lies at an arbitrary angle in the x - y plane, this technique is optimally suited to detect twists in buried magnetic layers. Although Hahn *et al.* used front-back reflectivity to study Fe/Gd multilayers [13], their differences in reflectivity result from the strong neutron absorption of the Gd when that material is closest to the incident beam. In our work absorption plays no role in the reflectivity, but there can still be a significant difference between front-back reflectivities.

Other experimenters measuring PNR have reported spirals in magnetic nanostructures [14,15], but the uniqueness of their models is in question because the reflectivity was measured from one surface only. Lohstroh [14] used the PNR method in which the neutrons are polarized along z instead of x . In this geometry nuclear and magnetic scattering are separated into the NSF and SF channels, respectively [16]. Differences between the SF reflectivities R^{+-} and R^{-+} signify a spiral with a unique chirality. Our sample should exhibit equal volumes of domains of clockwise and anticlockwise twists because the fields are

always along x . In this case, incoherent summation of the domain reflectivities produces identical SF reflectivities. Furthermore, in field-dependent studies of the spiral, fields $H \gtrsim 5$ mT applied in-plane along x would not preserve the neutron polarization along z .

Two recent refinements in PNR techniques yield additional information about the magnetic structure and thereby reduce the inherent ambiguity. One technique determines the phase of the neutron reflected from the magnetic film [17]. It relies on the homogeneity of the sample and fails in the presence of multiple chiral domains. The technique of zero-field neutron polarimetry extends the method used by Lohstroh [14] to unrestricted orientation of the neutron polarization [12,18], but it cannot be used to study the field development of the spiral.

Although simultaneous fitting of the front-back reflectivity provides an exclusion of other possible spin configurations, our fits to just the front reflectivity yield comparable nonzero ω . Back and front reflectivities were measured only at $H = 16$ and 26 mT. But given the placement of these fields on the hysteresis loop, we have confidence that the fits for the remaining fields, for which we presently have only front-surface reflectivity, provide a consistent picture of the demagnetization process.

Figure 2 shows the fitted spin structure for six of the measured fields, including the aligned state at 630 mT. The surface normal z is vertical in the figures. The red curves show the projection of the spirals into the $z = 0$ plane. The NiFe is near the top (purple through green) and the FePt is towards the bottom in yellow. X-ray

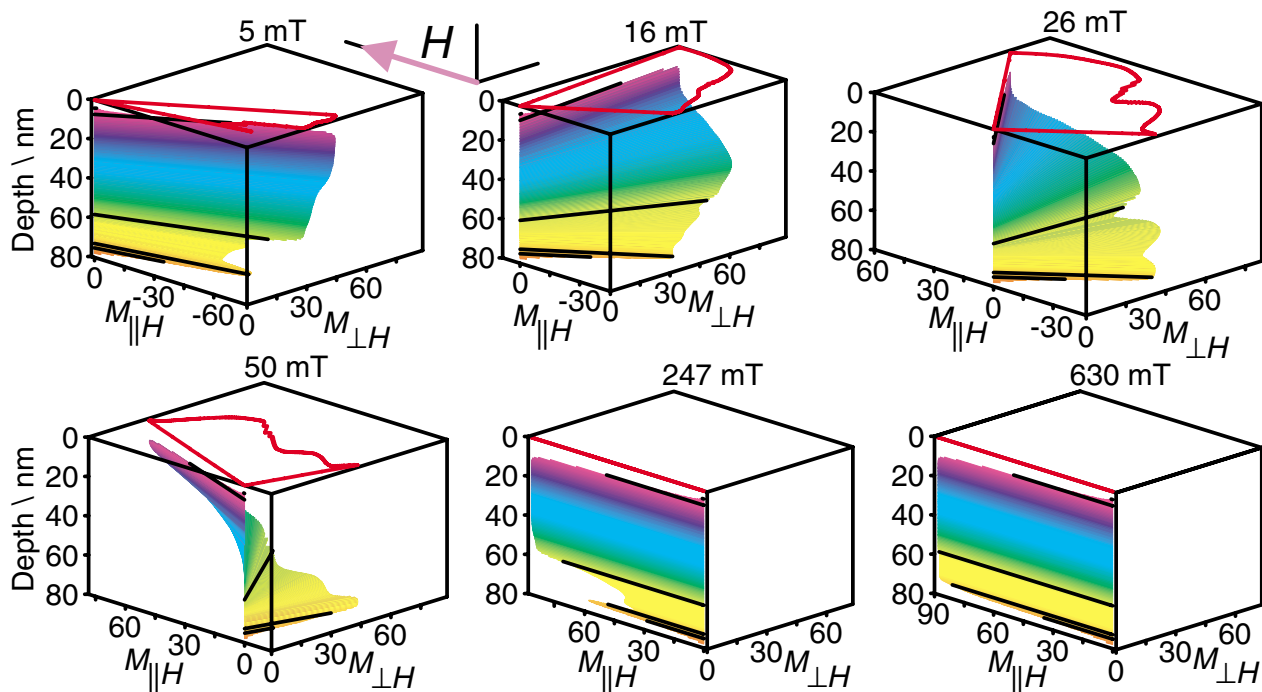


FIG. 2 (color). Magnetic structure from the fits at several fields. The NiFe is shown in purple through green. The FePt is shown in yellow. The Pt seed layer (with slight Fe contamination) is shown in orange. Heavy black lines separate the different layers of the film. The red curve is the projection of the spiral into the $z = 0$ plane. The field is applied in the direction shown.

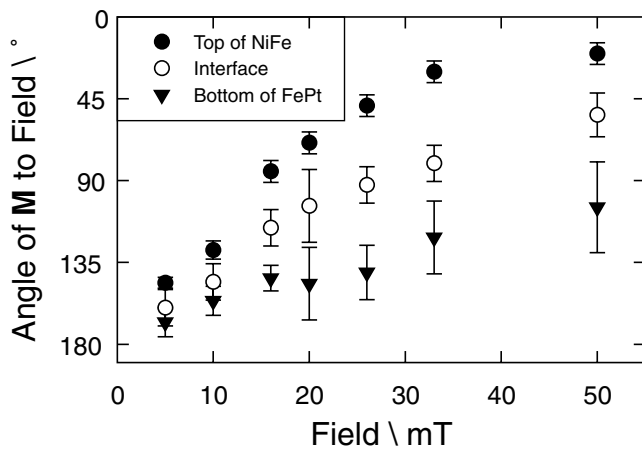


FIG. 3. The angle of the magnetization at the top of the NiFe (\bullet), the interface (\circ), and at the bottom of the FePt (\blacktriangledown).

reflectometry suggests the Pt seed layer, depicted at the bottom in orange, has some Fe diffused into it.

As the field increases from 5 through 50 mT, we see the spiral opens. Above 50 mT the spin-flip scattering disappears into the background and we fit the reflectivities assuming the moment lies entirely along $+x$. The fits are very sensitive to the orientation ϕ_s and the size of the magnetization in the NiFe. In the top two-thirds of the layer the magnetization is uniform with the value of bulk permalloy. We are also sensitive to the interfacial angle ϕ_{int} , and to a lesser extent the angle ϕ_h at the bottom of FePt. We are less sensitive to the thicknesses t_s and t_h of uniform moment orientation in either component. In the aligned state at 630 mT the FePt magnetization nearly equals that of bulk permalloy, which is consistent with measurements by Goto on similar FePt films [19]. For the other fields there is a consistent reduction in the FePt moment with variations which are not uniquely determined by the fits. These reductions may indicate that across the sample the polycrystal forms magnetic domains no wider than 100 μm (of the order of the coherence length of the neutrons). Alternatively, the FePt spins at these depths may be tilting out of the film plane (towards \mathbf{Q}).

Figure 3 shows the fitted angle at three depths in the sample: at the top of the NiFe, at the interface between NiFe and FePt, and at the bottom of the FePt. Our quantitative results for the interfacial angle directly confirm earlier MOKE studies [8] which suggest the twist involves the FePt, even for small reverse fields. Between 16 and 50 mT roughly half the twist lies in the hard layer, yet the bulk magnetization [8] suggests reversibility in this region. (The simple model of Kneller and Hawig [2] predicts irreversible behavior when the domain wall penetrates the hard ferromagnet.) Furthermore, the best fits to the reflectivity do not have the FePt pinned along the aligned field

direction with $\phi_h \equiv 180^\circ$. Instead, ϕ_h steadily increases with field. However, after inspecting the simulated reflectivity, we cannot yet rule out $\phi_h \equiv 180^\circ$, as predicted by the original models. With data from so many fields, we can confidently begin a comparison of the depth and field dependence of the angle with predictions of mean-field models [20]. These models must first be adapted to our polycrystalline sample [11].

In summary, in a simple extension of the typical PNR experiment, we have measured the reflectivity from the front surface and back surface of a spring-magnet bilayer. With double the number of simultaneously fitted measurements, we readily extract the magnetic spiral in the buried layers. With this new technique, coherent noncollinear structures can be easily detected, even in single-layer films. We used the technique to track the field evolution of the spiral in the bilayer. Contrary to our expectations for low field, reversible magnetization involves a portion of the hard ferromagnet. The technique is simple to implement and can be applied to a variety of current problems of domain wall formation perpendicular to and motion parallel to the scattering vector \mathbf{Q} .

*Electronic address: kevin.odonovan@nist.gov

- [1] A. E. Berkowitz and K. Takano, *J. Magn. Magn. Mater.* **200**, 552 (1999), and references therein; J. Nogués and I. K. Schuller, *J. Magn. Magn. Mater.* **192**, 203 (1999), and references therein.
- [2] E. F. Kneller and R. Hawig, *IEEE Trans. Magn.* **27**, 3588 (1991).
- [3] R. Skomski and J. M. D. Coey, *Phys. Rev. B* **48**, 15 812 (1993).
- [4] K. Mibu *et al.*, *Phys. Rev. B* **58**, 6442 (1998).
- [5] E. E. Fullerton *et al.*, *Phys. Rev. B* **58**, 12 193 (1998); E. E. Fullerton *et al.*, *J. Magn. Magn. Mater.* **200**, 392 (1999).
- [6] S. Mangin *et al.*, *Phys. Rev. B* **58**, 2748 (1998).
- [7] J. Unguris *et al.*, *Phys. Rev. Lett.* **67**, 140 (1991).
- [8] O. Hellwig *et al.*, *Phys. Rev. B* **62**, 11 694 (2000).
- [9] J. S. Jiang *et al.*, *IEEE Trans. Magn.* **35**, 3229 (1999).
- [10] C. F. Majkrzak, *Physica (Amsterdam)* **221B**, 342 (1996).
- [11] K. V. O'Donovan, J. A. Borchers, C. F. Majkrzak, O. Hellwig, and E. E. Fullerton (to be published).
- [12] A. Rühm *et al.*, *Phys. Rev. B* **60**, 16 073 (1999).
- [13] W. Hahn *et al.*, *Phys. Rev. B* **52**, 16 041 (1995).
- [14] W. Lohstroh *et al.*, *J. Magn. Magn. Mater.* **198-199**, 440 (1999).
- [15] S. Mangin *et al.*, *Physica (Amsterdam)* **276B-277B**, 558 (2000).
- [16] M. Blume, *Phys. Rev.* **130**, 1670 (1963).
- [17] J. Kasper *et al.*, *Phys. Rev. Lett.* **80**, 2614 (1998).
- [18] P. J. Brown *et al.*, *Proc. R. Soc. London A* **442**, 147 (1993).
- [19] T. Goto *et al.*, *J. Magn. Magn. Mater.* **198-199**, 486 (1999).
- [20] E. Goto *et al.*, *J. Appl. Phys.* **36**, 2951 (1965).